

THE EFFECT OF SHOT PEENING ON TRIBO-CORROSION CHARACTERISTICS OF ADDITIVELY MANUFACTURED Ti-6Al-4V USED IN THE MARINE INDUSTRY

K.A. Vella^a, J. Buhagiar^a, G. Cassar^a, L. Bonnici^a, M.M. Pizzuto^a, J. Chen^b, X.Y. Zhang^b, M.Y. Liu^b, Z.Q. Huang^b, A. Zammit^a

^a Department of Metallurgy and Materials Engineering, University of Malta, Msida, Malta – ann.zammit@um.edu.mt

^b School of Materials Science and Engineering, Southeast University, Nanjing, Jiangsu Province, China – j.chen@seu.edu.cn

Abstract

Ti-6Al-4V is a long-established titanium alloy, however, its use is often limited by its poor behaviour under friction conditions. Such behaviour is more pronounced in environments where corrosion occurs in conjunction with wear. This limitation can be mitigated through surface engineering techniques. In this investigation, the titanium substrates, manufactured via selective laser melting, were subjected to a shot peening treatment. The effect of the surface treatment on the microstructure, microhardness and roughness of the samples was studied via a number of characterisation techniques. To provide an insight into the corrosion-wear response, the samples were tested under reciprocating sliding wear conditions at an anodic potential in simulated ocean water. The shot-peened samples exhibited no improvement in the corrosion-wear resistance when compared to the untreated printed samples. Tribocorrosion calculations suggest degradation occurred due to mechanical wear with a marginal contribution from corrosion.

Keywords additive manufacturing, shot peening, tribocorrosion, hardness, roughness

Introduction

Ti-6Al-4V (Ti64) is a widely used titanium alloy having various ideal properties, such as high specific strength, low elastic modulus and good fatigue strength [1]. Furthermore, manufacturing the alloy via additive manufacturing is beneficial due to the provided ability of rapidly producing complex parts with minimal post-processing. The alloy's employment in the marine industry is not uncommon, especially since its use provides the ability of producing lightweight components having excellent corrosion resistance. However, the use of Ti64 is limited by its poor behaviour under friction conditions observed as, high unstable coefficients of friction with a tendency to gall and fret. Surface engineering techniques such as shot peening (SP) can be used to combat this limitation.

SP is a cold working process which induces beneficial residual compressive stresses at the surface via high-velocity impingement of shots, intended to increase the fatigue strength and reduce stress corrosion cracking. It has been recognized that the tribological performance of the shot peened component can be enhanced by the surface hardening and lubrication effects of the dimples [2]. However, the effect of SP on the tribocorrosion behaviour of additively manufactured Ti64 is not yet extensively studied. So far some authors have reported that the SP treatment decreased the material loss due to both wear and corrosion, others reported that the induced roughness has a negative effect on the corrosion-wear resistance [3], [4].

In the current investigation, the effect of this SP treatment on the corrosion-wear characteristics of a 3D printed Ti-6Al-4V alloy, was studied. This was done by subjecting an

untreated and a shot peened sample to linearly reciprocating ball-on-flat sliding wear testing conducted in simulated ocean water. The obtained wear tracks were characterised via profilometry and micrographic techniques, and material losses due to corrosion-wear were quantified. The samples were also analysed via microscopy, microhardness testing, profilometry and X-ray diffraction to investigate the effect of the surface treatment.

Experimental Methods

Sample preparation

The 20 mm diameter and 6 mm thick Ti64 samples were manufactured by selective laser melting (SLM) a Ti-6Al-4V powder, having a maximum particle size of 35 μm . The samples were printed layer by layer at a laser speed and power of 600 mms^{-1} and 100 W respectively, each layer having a thickness of 30 μm . The samples, having the composition listed in Table 1, were ground and polished up to a mirror finish. Prior to grinding and polishing, the SLM printed samples were heat treated, using a TAV Dualjet TPH-200 (Italy) furnace, in a nitrogen atmosphere till 800°C at a ramp rate of 5°C min^{-1} for 2 hours followed by furnace cooling.

Table 1. Composition of 3D printed Ti64 obtained by EDS analysis

	Ti	Al	V	Fe
wt%	Bal.	5.37	3.94	1.15

Surface treatments

The SP treatment was carried out using an Almen intensity of 0.24 mmA, 6 bar pressure and a nozzle-to-specimen distance of 100 mm. The samples were peened using Zirshot Z300 ceramic shots for a duration of 60 seconds to obtain 500% coverage.

Surface and near-surface characterisation

Micrographic analysis of the samples was carried out using the Carl Zeiss Axioscope 5 (Germany) optical microscope and the Carl Zeiss Merlin Gemini (Germany) scanning electron microscope (SEM) in conjunction with an Ametek EDAX (USA) energy dispersive spectroscopy (EDS) analyser. Prior to visualisation, the substrates were etched for 10 seconds using Kroll's reagent composed of 5% HF, 13.5% HNO₃ and 81.5% H₂O.

For phase analysis, X-ray diffraction was performed via the Bruker AXS D8 Advance (USA) machine. Scans were performed over a 2 θ range of 20° to 90° with a step size of 0.02° and a dwell time of 2 seconds using a CuK α radiation source. Stress measurements were obtained using the Rigaku Ultima VI (Japan) diffractometer. Measurements were taken at seven ψ tilts, from 0° to 60°, stresses were then obtained via the $\text{Sin}^2\psi$ method.

Surface roughness measurements were carried out via an AEP Technology NanoMap-500LS (USA) contact profilometer. Scans were performed over a distance of 2500 μm at 25 μms^{-1} and a resolution of 1 μm . Five scans were performed for each sample condition.

Using the Mitutoyo MVK-H2 (Japan) microhardness tester in conjunction with a pyramidal diamond indenter, Vickers microhardness measurements were obtained. A load of 100 gf was applied, the application lasting for 10 seconds. A series of five indentations were applied.

Tribocorrosion testing

For tribocorrosion testing, a Bruker UMT TriboLab (USA) set up with a reciprocating drive and a 3-electrode tribocorrosion cell was used. The cell was connected to a Gamry Interface 1000™ (USA) potentiostat to induce an anodic potential of 0.5 V with respect to the Ag/AgCl reference electrode. This potential ensures that all samples are in the passive regime. The cell was filled with approximately 150 ml of artificial seawater formulated in accordance with ASTM D1141-93 *Standard Practice for the Preparation of Substitute Ocean Water*. A 4.76 mm diameter Al₂O₃ counter-face was utilised. The voltage was induced for 600 seconds without sliding, for stabilisation, followed by sliding for 2000 seconds at a static Hertzian contact pressure of 678 MPa, frequency of 1Hz and a stroke length of 3.5 mm. During sliding, the

dynamic anodic current and COF values were recorded. Once sliding stopped, the anodic potential was applied for a further 600 seconds. All tests were repeated three times at room temperature.

Wear track characterisation

Following testing, elemental analysis of any debris and artefacts present was carried out. All wear track depths were measured via profilometry, each wear track measured using an average of three linear scans. From data collected during testing and measurements taken, the material loss rates were quantified [5].

Results and Discussion

Characterisation of samples

Following shot peening, the effect of grain refinement was observed. The grains appear denser at the surface and assume a basket-weave network further away as observed in Figure 1.

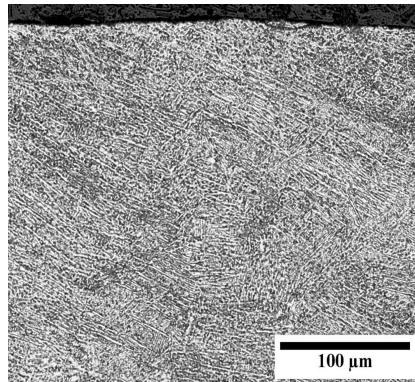


Figure 1. Low magnification micrograph of the cross-sectioned shot peened sample

As observed in Figure 2, a shift towards lower 2-theta values is observed for the printed and shot peened (SP) sample. This shift in the spectra is due to the induced compressive residual stresses, thus confirming that the peening treatment was effective. At the surface, a compressive residual stress (CRS) equivalent to 432 MPa was measured suggesting that a significant plastic deformation occurred. Similar stress magnitudes were measured by Zhang *et al.* [6] for SLM Ti64 following SP and furthermore, experienced no phase transformation. The stress magnitude is observed to be dependent on shot velocity and on the shot diameter. Impingement at higher speeds induces greater plastic deformation thus an increase in the CRS at the surface [6]. In the current study, no new peaks were detected thus, phase transformation due to SP also did not occur. It is likely that the peening intensity is too low to induce phase transformation. Moreover, broader and less intense peaks are observed for the SP sample as a consequence of the roughened surface as the surface asperities absorb the diffracted rays [7].

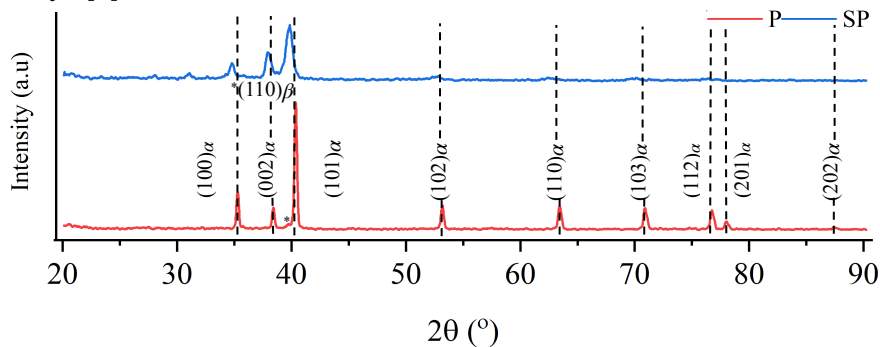


Figure 2. Peaks detected by X-ray diffraction

As observed in Table 2, the R_a and R_z roughness values were the highest for the samples which had been printed and subsequently shot peened (SP). This was expected due to the

roughening effect imparted by the SP treatment. The impact of shots results in sharp protrusions due to the interaction of the dimples.

Table 2. Hardness and roughness measurements. For both measurements, uncertainty is represented by 95% confidence interval for a population size of 5.

Sample	Hardness (HV _{0.1})	Roughness	
		R _a (μm)	R _z (μm)
P	331 ± 2.31	0.05 ± 0.01	1.33 ± 0.52
SP	375 ± 4.47	1.47 ± 0.13	11.60 ± 0.95

Following SP, the hardness of the printed sample increased by 13% thus confirming the occurrence of a degree of work hardening. A similar increase is observed by Zhang *et al.* [6] for SP SLM Ti64. Such hardening is due to grain refinement, which results in an increase in grain boundaries and thus a greater hindrance to dislocation movement, and induced compressive residual stresses. The hardness values were highest at the surface and decreased gradually to the bulk hardness resulting in an affected depth ranging from 180 to 200 μm; also in line with what was observed by other authors [6].

Corrosion-wear response of untreated and treated AM Ti-6Al-4V

Dynamic anodic current and coefficient of friction measurements

For both sample conditions, upon sliding, an increase in anodic current was observed which dropped back to initial values once sliding stopped. This increase is due to the removal of the passive film exposing the underlying substrate to oxidation [8]. Both samples underwent Type I corrosion-wear which is the removal or damage of the passive layer present at the coating surface and its subsequent re-passivation. This mechanism is reflected in the constant fluctuations of corrosion-current, corresponding to the continuous re-passivation and de-passivation, as observed in Figure 3(a,b).

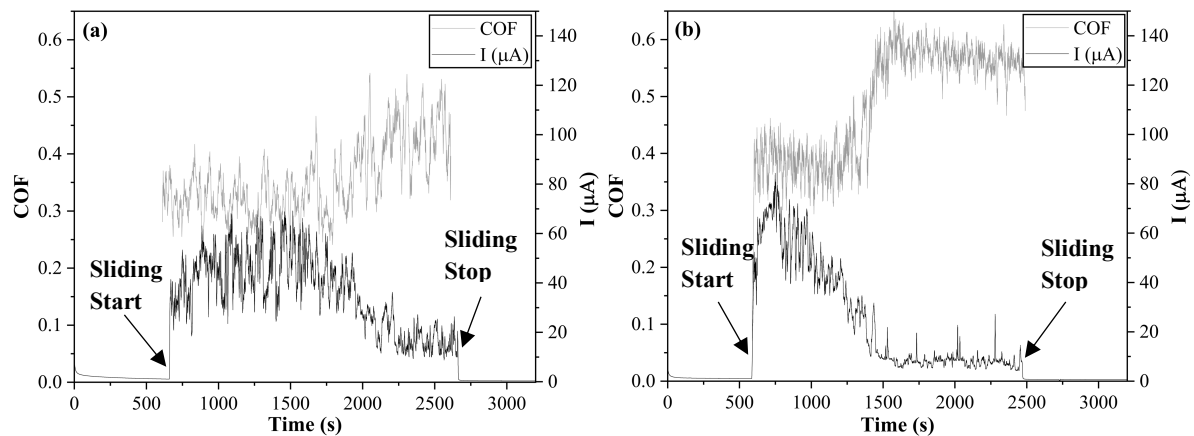


Figure 3. Dynamic anodic current and COF plots a) printed and b) printed + shot peened Ti-6Al-4V

Furthermore, as observed, both the P and SP sample exhibited a similar behaviour which was observed for all three repeats carried out for both sample conditions. This decrease in current, which implies a decrease in the amount of new substrate exposed to the electrolyte, is simultaneously accompanied with an increase in the coefficient of friction (COF). This behaviour is attributed to the oxidised areas formed on the surface, confirmed to be composed of TiO₂ by EDS analysis. These form due to the strong adhesion between the substrate and the ceramic ball at asperities which results in high frictional forces. With sliding, the asperities are removed resulting in generation of debris, which is either compacted into re-adhered material or free third body particles contributing to abrasion [8]. Thus, these patches protect the surface from being exposed to the corrosive solution and hence from Type I corrosion-wear. Therefore, the current values decreased greatly. However, these patches also result in

an uneven wear track and increase the COF due to roughening the track [8], [9]. This behaviour could also be related to the formation of asperities which decrease the contact area. Thus, the contact pressure at such areas increases resulting in roughening. Meanwhile, due to a decrease in contact area, less area is being exposed to dissolution thus, the decrease in the current values [10].

For the SP sample, currents as high as 80 μA were recorded immediately upon sliding, suggesting that the substrate was exposed at once and that the SP treatment was ineffective. Moreover, the overall high COF values observed are typical for SP treated Ti64 since the treatment increases the surface roughness [11]. This increased roughness was most likely detrimental to the tribocorrosion behaviour. Several spikes, once current values stabilised at lower values, were also observed (Figure 3b). Such spikes are related to the development of wear particles where their formation results in de-passivation and subsequent re-passivation of the substrate [12].

Material Losses

Figure 4 depicts a plot of the material losses calculated from the anodic current and wear track depth measurements. From the plot no significant difference between the material losses the P and SP sample can be observed. Thus, the SP treatment appears to be ineffective.

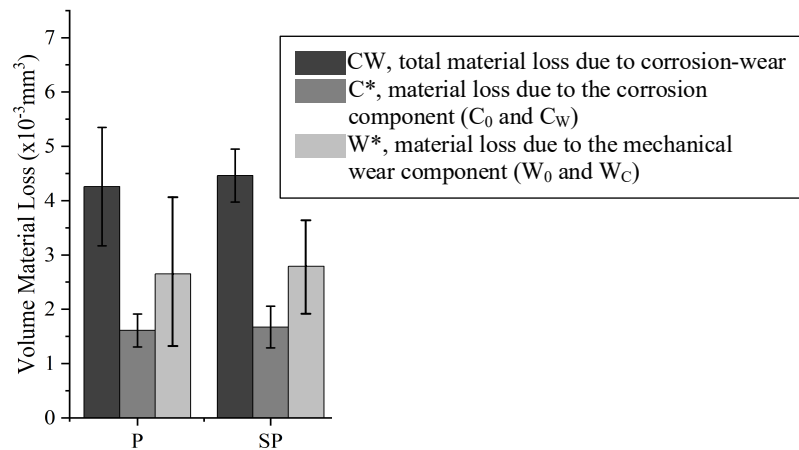


Figure 4. Volume material losses of the printed and printed and shot peened samples where, $CW = W^* + C^*$. Uncertainty deduced from minimum and maximum values obtained and based on a population size of 3.

The ratio of the loss due to the corrosion component and due to the wear component (C^*/W^*) provides an insight in the dominant degradation mechanisms present [8],[13]. The ratios obtained were 0.61 ± 0.20 and 0.60 ± 0.12 for the P and SP sample respectively. Since both values are between 0.1 and 1, this suggests that synergism is present and the most dominant mechanism is wear-corrosion. Therefore, the greatest losses are caused by the total mechanical wear component, which is also reflected in the results obtained. The former contributed to $62 \pm 7\%$ and $63 \pm 4.5\%$ of the corrosion-wear for the P and SP samples respectively. However, this method does not clearly identify whether the loss was due to pure mechanical wear (W_0) or due to mechanical wear due to corrosion (W_C).

Mechanical wear occurred via abrasive and adhesive mechanisms. Abrasive wear was evidenced by thencing in the direction of the sliding direction. Whilst, adhesive wear was evidenced by micro-asperity shearing. The developed oxidation patches were also a consequence of adhesion. Its occurrence was also reflected by the unstable COF and high wear rates of the P and SP samples.

Conclusions

The following conclusions can be drawn from the results obtained when studying the effect of shot peening on 3D printed Ti-6Al-4V substrate:

1. Broader X-ray diffraction peaks shifted toward lower 2-theta values confirming the occurrence of grain refinement and presence of residual stresses due to the SP treatment. A compressive surface stress equivalent to 432 MPa was obtained.
2. Due to the shot impingement, the R_a and R_z values of the P sample increased by approximately 3 orders and 1 order of magnitude respectively.
3. Following SP, the hardness of the P sample increased by 13% and the affected depth reaches a maximum of 200 μm .
4. The corrosion-wear resistance did not increase following SP. The similar behaviour of the P and SP sample indicates that the peening treatment was ineffective in this case.
5. Both sample conditions obtained a C^*/W^* ratio in the range of 0.1 to 1 confirming that synergism was present and the wear-corrosion mechanism was the most dominant.
6. Type I corrosion-wear was observed. Mechanical wear was observed as abrasion in term of grooves. Adhesive wear was evidenced by micro-asperity shearing and reflected by the unstable COF values and significant wear rates obtained.

Acknowledgements

The research carried out is part of a Sino-Malta project regarding Surface Engineering of Additive Manufactured (SEAM) parts used in marine transportation and was possible due to funding provided by the Malta Council for Science and Technology (MCST).

References

- [1] A. Loureiro *et al.*, "Properties and Applications of Titanium Alloys: A Brief Review," *Rev. Adv. Mater. Sci.*, no. 32, pp. 14–34, 2012.
- [2] A. Zammit, "Shot Peening of Austempered Ductile Iron," in *Advanced Surface Engineering Research*, M. A. Chowdhury, Ed. Rijeka: IntechOpen, 2018.
- [3] Y. Sun and R. Bailey, "Improvement in tribocorrosion behavior of 304 stainless steel by surface mechanical attrition treatment," *Surf. Coat. Technol.*, vol. 253, pp. 284–291, Aug. 2014.
- [4] A. S. Hammood *et al.*, "Tribocorrosion Behaviour of Ti-6Al-4V Alloy in Biomedical Implants: Effects of Applied Load and Surface Roughness on Material Degradation," *J. Bio-Tribo-Corros.*, vol. 5, no. 4, Dec. 2019.
- [5] B. Mallia and P. A. Dearnley, "The corrosion-wear response of Cr-Ti coatings," *Wear*, vol. 263, pp. 679–690, Sep. 2007.
- [6] Q. Zhang *et al.*, "Microstructure change and corrosion resistance of selective laser melted Ti-6Al-4V alloy subjected to pneumatic shot peening and ultrasonic shot peening," *Surf. Topogr. Metrol. Prop.*, vol. 10, no. 1, Mar. 2022.
- [7] A. Zammit *et al.*, "Enhancing surface integrity of titanium alloy through hybrid surface modification (HSM) treatments," *Mater. Chem. Phys.*, vol. 279, p. 125768, Mar. 2022.
- [8] F. Toptan *et al.*, "Corrosion and tribocorrosion behaviour of Ti6Al4V produced by selective laser melting and hot pressing in comparison with the commercial alloy," *J. Mater. Process. Technol.*, vol. 266, pp. 239–245, Apr. 2019.
- [9] I. Çaha *et al.*, "Corrosion and tribocorrosion behaviour of titanium nitride thin films grown on titanium under different deposition times," *Surf. Coat. Technol.*, vol. 374, pp. 878–888, 2019.
- [10] R. Chetcuti *et al.*, "Tribocorrosion response of duplex layered CoCrMoC/CrN and CrN/CoCrMoC coatings on implant grade 316LVM stainless steel," *Surf. Coat. Technol.*, vol. 384, p. 125-313, Feb. 2020.
- [11] D. G. Bansal *et al.*, "Surface engineering to improve the durability and lubricity of Ti-6Al-4V alloy," *Wear*, vol. 271, no. 9, pp. 2006–2015, 2011.
- [12] D. Landolt, "Electrochemical and materials aspects of tribocorrosion systems," *J. Phys. Appl. Phys.*, vol. 39, no. 15, pp. 3121–3127, Aug. 2006.
- [13] M. J. Runa *et al.*, "Tribocorrosion response of the Ti6Al4V alloys commonly used in femoral stems," *3rd Int. Conf. Tribocorrosion – Atlanta 2012*, vol. 68, pp. 85–93, Dec. 2013.